IEEE Access
Multidisciplinary | Rapid Review | Open Access Journal

Date of publication xxxx 00, 0000, date of current version xxxx 00, 0000.

Digital Object Identifier 10.1109/ACCESS.2017.Doi Number

A Simple and Accurate Method for Extracting Super Wideband Electrical Properties of the Printed Circuit Board

YI-WEN WU[1], (Student Member, IEEE), ZHANG-CHENG HAO[1,2], (Senior Member, IEEE), MING-CUI TAO[1], XIANG WANG[1], (Student Member, IEEE), and JIA-SHENG HONG[3], (Fellow, IEEE)

[1]State Key Laboratory of Millimeter-wave, School of Information Science and Engineering, Southeast University, Nanjing 210096, China
[2]Purple Mountain Laboratories, Nanjing, China
[3]School of Engineering and Physical Sciences, Heriot-Watt University, Edinburgh, EH14 4AS, U.K.

Corresponding author: Zhang-Cheng Hao (e-mail: zchao@seu.edu.cn).

This work was supported in part by the National Natural Science Foundation of China 61471118 and 61501114.

ABSTRACT In order to accurately design microwave, millimeter-wave components and circuits, a simple and accurate method for extracting extremely wideband characteristics of the printed-circuit-board (PCB), including relative dielectric constant, dielectric loss tangent and equivalent copper conductivity, is proposed and validated in this paper. By properly designing the circular substrate integrated waveguide (CSIW) cavity to let its resonating modes distribute within a wide frequency band, extremely broadband properties of the PCB can theoretically be extracted with only one pair of CSIW cavities. The proposed method overcomes the limitations of conventional methods that only support narrowband applications, require a large number of cavities and have relatively large errors. Experiments show that the proposed method is able to extract, accurately and efficiently, the 8-110 GHz characteristics of a TLY-5Z substrate based PCB. And, the extracted results are verified by designing and measuring a fourth-order Chebyshev filter at X band.

INDEX TERMS Dielectric constant, dielectric loss tangent, equivalent conductivity, circular substrate integrated waveguide (CSIW) cavity, wideband characteristics.

I. INTRODUCTION

The investigation of microwave, millimeter-wave or terahertz components and circuits based on various technologies such as the printed-circuit-board (PCB) technology [1]-[7] and the low-temperature co-fired ceramic (LTCC) technology [8]-[14] has drawn tremendous attentions due to rapid development of modern wireless systems recently. The dielectric and metal characteristics play an important role in the design of microwave and millimeter-wave components, especially at high millimeter-wave frequency. However, these characteristics provided by PCB manufactures are usually only accurate for narrowband and low frequency applications. To this end, many efforts have been made to measure those characteristics for the accurate design of millimeter-wave or terahertz components, including the transmission/reflection method [15]-[16] and the resonator method [17]-[22]. The substrate integrated waveguide (SIW) technology has come into notice in recent years because of the merits of easy integration, high unloaded quality factor (Q-factor) and low cost [23]-[29]. In addition, the leakage loss is negligible with suitable spacing and size of metallized via-holes. Hence, it has been adopted to extract the characteristics of PCB [17]-[21]. Generally, the transmission/reflection method can be used to extract the wideband electrical characteristics of PCB with a relatively low accuracy. Compared to the transmission/reflection method, the resonator method has a higher accuracy [18]. However, the traditional resonator methods based on rectangular substrate integrated waveguide (RSIW) resonators suffer from single frequency or narrowband applications. For example, the frequency bandwidth must meet the limitation that: f_H/f_L <2.12 [18]-[21].To extract wideband material characteristics, a large number of cavities, which are designed to resonant at different frequencies, have to be used in the experiment. Hence, it not only needs a complex design for a large number of cavities, but also requires tedious measurements for each cavity, which leads to an increased measurement error as well, especially for millimeter-wave or terahertz application. For example, tens or

This article has been accepted for publication in a future issue of this journal, but has not been fully edited. Content may change prior to final publication. Citation information: DOI 10.1109/ACCESS.2019.2911616, IEEE Access

dozens of cavities have to be adopted in the experiment in order to obtain the 8-60 GHz characteristics of PCB [19] [20].

For accurate design of microwave, millimeter-wave components and circuits, a simple and accurate method based on the resonator method is proposed for extracting extremely wideband characteristics of PCB by using CSIW cavities in this paper. The principle for extracting equivalent metal conductivity, dielectric loss tangent and relative dielectric constant is discussed in detail in the Section II. In Section III, the proposed method is demonstrated by experiments for extracting the 8-110 GHz characteristics of a Taconic TLY-5Z based PCB with high efficiency and accuracy, and detailed discussions are presented in the Section IV. Then, the results are verified by a fourth-order Chebyshev filter at X band in Section V. Finally, the conclusion is summarized in the Section VI.

II. EXTRACTING PRINCIPLE

It is well known that in order to extract the electrical characteristics of a material by using the resonator method with a high accuracy, the Q-factor of the employed resonator is expected to be as high as possible. In theory, various types of PCB resonators could be used for the PCB material characteristics extraction, including the microstrip resonator, the coplanar waveguide resonator, the stripline resonator as well as the SIW resonator [17]-[22]. Compared with the other types of PCB resonators, the SIW resonator may be the best choice because it can provide much high quality factors even at W-band or above [7]. In addition, among various types of SIW resonators, the CSIW cavity, which has a higher Q-factor, better fabrication tolerance and a more compact size than the other types of SIW resonators [30], is more attractive for the high frequency material characteristics extraction. In addition, CSIW cavity has a more broadband frequency bandwidth compared with RSIW resonators, because the appearance of resonating modes in CSIW resonator follows the rule of the root of Bessel function shown in Fig. 2 which ensures a good selection of resonating modes for broadband and accurate characteristics extraction of PCB. Therefore, the CSIW resonators with weak excitations shown in Fig.1 with different substrate thicknesses are deployed in the proposed method. Different to the traditional resonator method which only utilizes one resonating mode to extract electrical characteristics [19], numerous resonating modes of the CSIW cavity are deployed in the proposed method. Since all resonating modes, excluding the degenerate mode, resonate at different frequencies and are distributed within an unlimited frequency band, the higher order modes are exploited to extract wider frequency band electrical characteristics of PCB [31].

As shown in Fig.1, grounded coplanar waveguide (GCPW) provides weak excitations for CSIW resonators due to the good dispersion characteristics in millimeter-wave bands. And the transmission loss from GCPW to the CSIW resonator hardly affects the Q-factor of CSIW resonator because of the

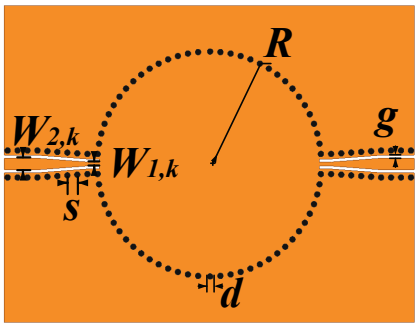

FIGURE 1. Layout of the adopted CSIW cavity for extracting wideband PCB material characteristics.

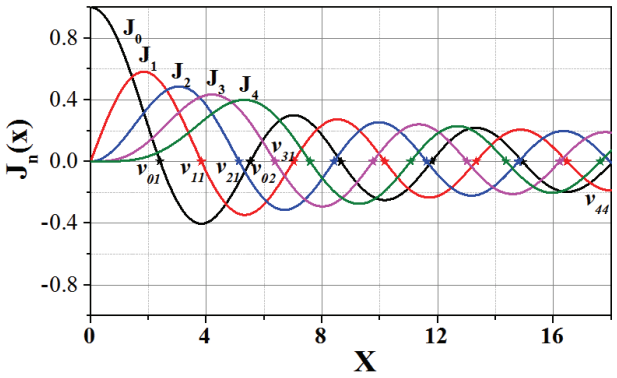

FIGURE 2. High order Bessel function curves.

weak excitations. Supposing the substrate thickness is less than one half-wavelength, the CSIW resonator only supports $TM_{m,n,0}$ resonating modes because the $\emptyset$ direction component of the $TE_{m,n,k}$-mode electrical field cannot be supported due to the discontinuity of metallic vias which form the sidewall of the circular SIW resonator. Then, the resonant frequency can be expressed as [32]:

$$f_{TM_{m,n,0}} = \frac{C_0}{\sqrt{\varepsilon_r}} \frac{v_{m,n}}{2\pi R_{eff}} \tag{1}$$

where C_0 is the speed of light in vacuum, R_{eff} is the effective radius of the CSIW resonator, $v_{m,n}$ is the *nth* root of the Bessel function of order m, and ε_r is the equivalent relative permittivity of the substrate.

From (1), it can be seen that once the effective radius, R_{eff}, of the CSIW resonator is determined, the operating frequency can be calculated by properly choosing the operating mode. Two CSIW resonators with different thicknesses are deployed in the proposed method. These two resonators have the same $TM_{m,n,0}$ (m=0..M_0, n=1..N_0) resonating modes. By measuring the loaded Q-factor of all those modes, their unloaded Q-factor can be deduced. Then the electrical characteristics of PCB can be extracted by individually comparing the unloaded Q-factors of each pair of corresponding resonating modes of the two CSIW resonators. Consequently, the operating frequency bandwidth covers from the resonating frequency of the fundamental mode to that of the highest selected mode. It should be mentioned that the proposed method is especially suitable for high millimeter-wave frequency extraction due to

the high-order resonating mode has a much higher Q-factor than that of the fundamental resonating mode. The detailed extracting process is explained in the following sections.

A. DETERMINING THE RADIUS OF THE CSIW RESONATOR

The radius of the CSIW resonator is related to the radius of a circular waveguide resonator, i.e. R_{eff}. As can be seen from (1), once the lowest operating frequency f_L of the material characteristics under extraction is preassigned and the initial relative dielectric constant is given by the manufacture, the equivalent radius R_{eff} of the CSIW resonator can be initially obtained from the relationship of the resonating frequency of the fundamental mode, i.e., the $TM_{0,1,0}$ mode, and R_{eff}, as (2) [32]. Then the frequency interval ($\Delta f_{m1,n1;m2,n2}$) between two adjacent modes ($TM_{m1,n1}$ and $TM_{m2,n2}$) of the material characteristics under extraction is calculated according to (3). Generally, a higher mode at the lowest frequency leads to a narrower bandwidth and a smaller frequency interval. Because some neighboring high-order modes are too close to each other in higher frequency band, which is difficult to distinguish between them. In order to extract broadband characteristics of PCB, the fundamental mode is selected as the first mode.

$$R_{eff} = \frac{C_0}{\sqrt{\varepsilon_r}} \frac{v_{m,n}(or\ v_{0,1})}{2\pi f_L(or\ f_{TM_{0,1,0}})};\ v_{0,1} = 2.405 \tag{2}$$

$$\Delta f_{m1,n1;m2,n2} = \frac{C_0}{\sqrt{\varepsilon_r}} \frac{v_{m2,n2} - v_{m1,n1}}{2\pi R_{eff}} \tag{3}$$

$$\frac{h}{R_{eff}} \le 2.1 \tag{4}$$

$$2R_{eff} = 2\mathrm{R} - \frac{d^2}{0.95s} \tag{5}$$

In addition, to support the fundamental mode, the $TM_{0,1,0}$ mode, the thickness of the substrate should satisfy (4) [32], and then an empirical relationship in (5) between the physical radius and the equivalent radius of the CSIW resonator can be obtained by the guidelines of RSIW [33].

B. UNLOADED Q-FACTOR OF THE CSIW RESONATOR

Theoretically, all the resonating modes of the CSIW resonator can be adopted for the material characteristics extraction. However, considering the planar excitation topology and easy measurement, only $TM_{m,n,0}$-mode is deployed in the extraction. The electromagnetic field of $TM_{m,n,0}$-mode in a CSIW resonator can be expressed as [34]:

$$\begin{aligned} E_\rho &= E_\varphi = H_z = 0 \\ E_z &= 2k_c^2 D J_m(k_c\rho)\cos(m\varphi) \\ H_\rho &= -j\frac{2\omega\varepsilon m}{\rho} D J_m \sin(m\varphi) \\ H_\varphi &= -j2\omega\varepsilon k_c J'_m(k_c\rho)\cos(m\varphi) \\ k_c &= \frac{v_{m,n}}{R} \end{aligned} \tag{6}$$

where m=0, 1, 2⋯; n=1, 2, 3⋯.

The unloaded Q-factor ($Q_{u_{m,n}}$) of the $TM_{m,n,0}$-mode can be expressed as [18]:

$$\frac{1}{Q_{u_{m,n}}} = \frac{1}{Q_{D_{m,n}}} + \frac{1}{Q_{c1_{m,n}}} + \frac{1}{Q_{c2_{m,n}}} \tag{7}$$

where $Q_{c1_{m,n}}$ is resulting from the conductor loss of the metallic-via sidewall of the CSIW resonator, $Q_{c2_{m,n}}$ represents the conductor loss from top and bottom surfaces of the CSIW resonator, and $Q_{D_{m,n}}$ is associated with the loss from the dielectric material, which can be represented as tanδ of the dielectric material.

In the measurement, weak coupling circuits shown in Fig. 1 can be used to extract the unloaded Q-factor $Q_{u_{m,n}}$ from the loaded Q-factor $Q_{L_{m,n}}$ and the coupling coefficients of the input/output ports as following [21]:

$$\begin{aligned} Q_{u_{m,n}} &= Q_{L_{m,n}}\left(1 + \beta_{1_{m,n}} + \beta_{2_{m,n}}\right) \\ Q_{L_{m,n}} &= \frac{f_{TM_{m,n,0}}}{\Delta f_{m,n,0}} \\ 2\beta_{1_{m,n}} &= \frac{S_{21,m,n}}{1 - S_{21,m,n}}\, i = 1,2. \end{aligned} \tag{8}$$

where $Q_{L_{mn}}$ is the loaded Q-factor for the $TM_{m,n,0}$ mode, $S_{21,m,n}$ is the magnitude of the transmission coefficient at resonant frequency, $f_{TM_{m,n,0}}$ is the resonating frequency of the $TM_{m,n,0}$-mode, and $\Delta f_{m,n,0}$ is the 3-dB bandwidth of the transmission coefficient. β_{1mn} and $\beta_{2m,n}$ are the coupling coefficients, which are almost equal due to the symmetrical structures in Fig.1 when the loss of material is not so serious. Then, the $Q_{u_{m,n}}$ can be extracted by (9)

$$Q_{u_{m,n}} = \frac{f_{TM_{m,n,0}}}{\Delta f_{m,n,0}} \frac{1}{1 - S_{21,m,n}} \tag{9}$$

The conductive loss includes the loss from the metallic-via sidewall, and top and bottom surfaces of the CSIW resonator. It can be expressed by using the conductive quality factor Q-factor, i.e. Q_c as:

$$\frac{1}{Q_{c_{m,n}}} = \frac{1}{Q_{c1_{m,n}}} + \frac{1}{Q_{c2_{m,n}}} \tag{10}$$

The $\mathrm{Q_{c_{m,n}}}$, $Q_{c1_{m,n}}$ and $Q_{c2_{m,n}}$ can be calculated using the definition of Q-factor:

$$\begin{aligned} Q_c &= \omega \frac{W}{P_{L1} + P_{L2}} \\ W &= (W_e)_{max} = \frac{h\varepsilon}{2}\int_0^{R_{eff}}\int_0^{2\pi} |E_z|^2 \rho d\rho d\varphi \\ P_{L1} &= \frac{1}{2} R_s h \int_0^{2\pi} |H_\varphi|^2_{\rho=R_{eff}} + |H_\rho|^2_{\rho=R_{eff}} d\varphi \\ P_{L2} &= \frac{1}{2} R_s \int_0^{R_{eff}}\int_0^{2\pi} |H_\varphi|^2 + |H_\rho|^2 d\rho d\varphi \end{aligned} \tag{11}$$

And, it can be expressed as

$$\begin{aligned} \frac{1}{Q_{c_{m,n}}} = \frac{1}{Q_{c1_{m,n}}} + \frac{1}{Q_{c2_{m,n}}} &= \sqrt{\frac{\varepsilon}{\mu}}\frac{2R_s k}{v_{m,n}} + \sqrt{\frac{\varepsilon}{\mu}}\frac{2R_s}{v_{m,n}}\frac{R_{eff}}{h} \\ \mathrm{k} &= \frac{dN}{2R_{eff}} q_1 \end{aligned} \tag{12}$$

where N is the number of metallic vias of the CSIW sidewall, d is the diameter of the metallic-via, R_{eff} is the effective radius of the CSIW resonator and R_s is the resistivity of metal surface. Since the currents of the resonating electromagnetic fields are non-uniformly distributed along the surface of each metallic-via, i.e. the inner surface has much stronger currents than that of the outer surface, an empirical coefficient of q_1=0.53 is used

This article has been accepted for publication in a future issue of this journal, but has not been fully edited. Content may change prior to final publication. Citation information: DOI 10.1109/ACCESS.2019.2911616, IEEE Access

TABLE I
DIMENSIONS OF THE CSIW RESONATORS (Unit: MM)

$W_{1,1}$	$W_{2,1}$	$W_{1,2}$	$W_{2,2}$	s	d	R	Gap
0.45	0.58	0.5	0.97	0.5	0.3	9.87	0.15

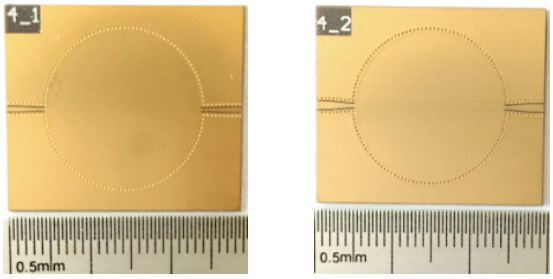

(a) (b)

FIGURE 3. Photographs of the fabricated prototypes for the 8-60 GHz extraction. (a) h_1 = 0.254 mm; (b) h_2 = 0.508 mm.

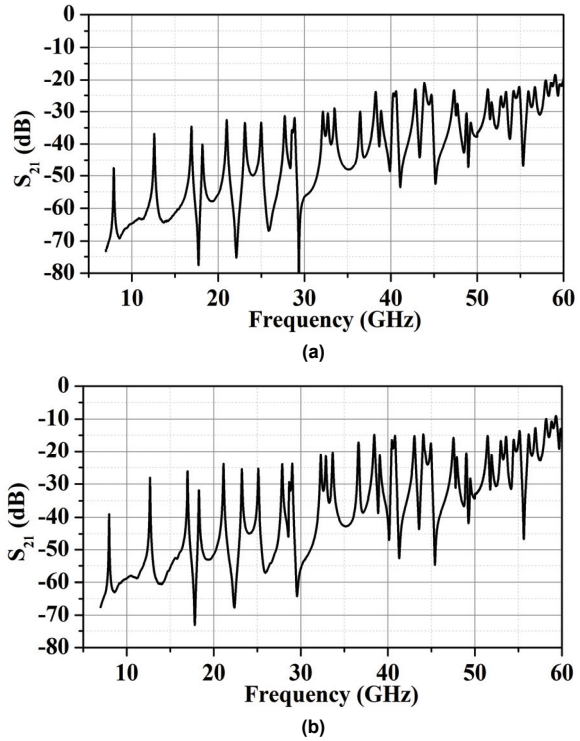

FIGURE 4. Measured transmission coefficients of CSIW cavities. (a) h_1 = 0.254 mm; (b) h_2 = 0.508 mm.

to represent the surface utilization ratio of metallic vias in the sidewall.

Based on above discussions, the unloaded Q-factor ($Q_{um,n}$) of the $TM_{m,n,0}$-mode in a CSIW resonator can be explicitly expressed as:

$$Q_{u_{m,n}} = tan\delta + \sqrt{\frac{\varepsilon}{\mu}}\frac{2R_s k}{v_{m,n}} + \sqrt{\frac{\varepsilon}{\mu}}\frac{2R_s}{v_{m,n}}\frac{R_{eff}}{h} \quad (13)$$

C. EFFECTIVE CONDUCTIVITY OF THE METAL

Two CSIW cavities with different heights, i.e., h_1 and h_2, have been used to extract the characteristics of PCB. Supposing the two unloaded Q-factor, i.e., $Q_{u1m,n}$ and $Q_{u2m,n}$, are measured with the circuit model shown in Fig.1, the conductor loss can

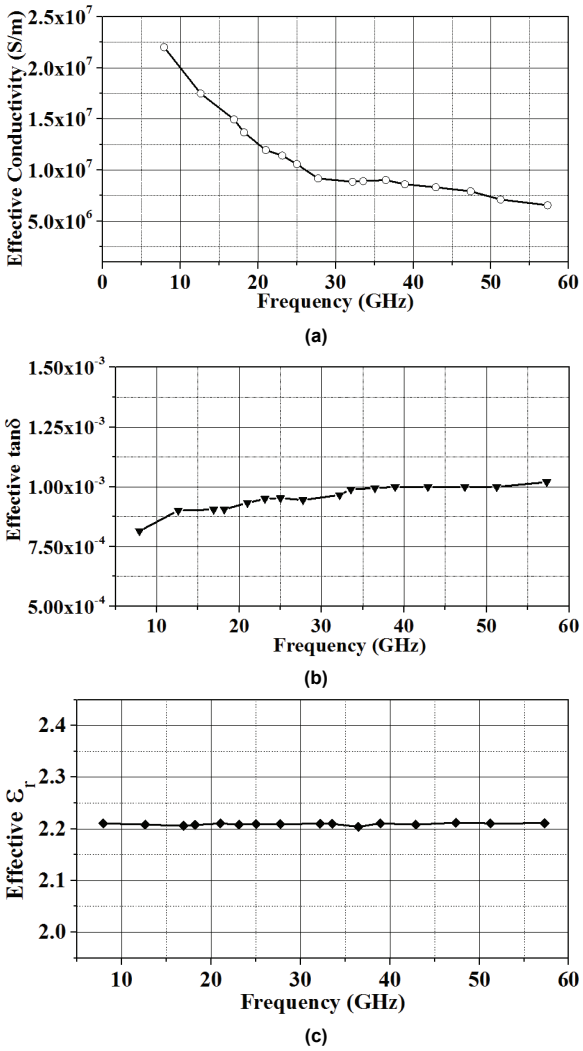

FIGURE 5. Extracted equivalent dielectric properties and conductivity of a TYL-5Z PCB within 8-60 GHz; (a) conductivity; (b) dielectric loss tangent; (c) relative dielectric constant from h=0.508 mm thick substrate.

be obtained by subtracting (13) with different thicknesses, and then

$$R_s = \frac{v_{m,n}}{2R_{eff}}\sqrt{\frac{\mu}{\varepsilon}}\frac{Q_{u2m,n}-Q_{u1m,n}}{Q_{u2m,n}Q_{u1m,n}}\frac{h_2-h_1}{h_2h_1} \quad (14)$$

where ε is the equivalent dielectric permittivity which can be extracted from the resonating frequency of the $TM_{m,n,0}$-mode, as shown in the next part, and $\mu = \mu_0 = 4\pi \times 10^{-7} H/m$ for a non-magnetic material. Considering the relationship between effective conductivity and equivalent resistivity of metal surfaces in (15), the equivalent conductivity can be extracted and expressed as (16):

$$R_s = \sqrt{\frac{\omega_{mn}\mu}{2\sigma}},\ \omega_{mn} = \frac{2\pi}{\lambda_{mn}\sqrt{\mu\varepsilon}},\ \lambda_{mn} = \frac{2\pi R_{eff}}{v_{mn}} \quad (15)$$

$$\sigma_{eff} = \frac{4\pi f_{TM_{mn0}} R_{eff}^2}{v_{mn}^2}\varepsilon\left(\frac{Q_{u2}Q_{u1}}{Q_{u2}-Q_{u1}}\right)^2\left(\frac{h_2-h_1}{h_2h_1}\right)^2 \quad (16)$$

D. EXTRACTING THE COMPLEX PERMITTIVITY OF THE DIELECTRIC SUBSTRATE

If the effective conductivity is obtained as discussed in the part C, the equivalent dielectric loss tangent can be deduced by substituting the resistivity of metal surface, R_s, into (13), and can be expressed as:

$$\tan\delta = \frac{1}{h_2-h_1}\left[\frac{h_2}{Q_{u2}}\left(k+\frac{h_2}{R_{eff}}\right)-\frac{h_1}{Q_{u1}}\left(k+\frac{h_1}{R_{eff}}\right)\right] \quad (17)$$

On the other hand, with the measurement of resonant frequencies of the TM_{mn0} mode, the equivalent relative dielectric constant at resonating frequency can be obtained and expressed as (18):

$$\varepsilon_r = \frac{C_0^2 v_{mn}^2}{f_{TMmn0}^2 4\pi^2 R_{eff}^2} \quad (18)$$

III. EXPERIMENTAL RESULTS

In this section, the proposed method has been used to extract the 8-110 GHz equivalent dielectric characteristics and conductivity for PCB. As a typical substrate for the design of microwave and millimeter-wave components, the Taconic TLY-5Z substrate is adopted in the commercial PCB fabrication process. According to the manufacture [35], the substrate has a relative dielectric constant of 2.2 ± 0.04 and a loss tangent of 0.001 at 1.9 GHz. The 0.035 mm thick copper is used as metal material in the PCB process for the fabrication of the circuits. Considering the measuring limitation, we divide the 8-110 GHz frequency band into three parts, i.e. 8-60 GHz, 60-75 GHz and 75-110 GHz, and extract the equivalent dielectric characteristics and conductivity for those three frequency bands individually. For 8-60 GHz frequency band, a pair of CSIW resonators with 0.254 mm and 0.508 mm thickness have been measured by using the Anritsu Test Fixture SC5225 [36], and the conventional waveguide interface is used to measure the responses of a pair of CSIW resonators for the other two frequency bands, respectively. This is because that the highest operating frequency of the Anritsu Test Fixture SC5225 is 60 GHz. The detailed extraction process will be discussed in the following parts.

A. EXTRACTION OF THE ELECTRICAL PROPERTIES OF THE TLY-5Z PCB WITHIN 8-60 GHZ

To extract the 8-60 GHz equivalent dielectric characteristics and conductivity, the resonating frequency of the fundamental mode, i.e. $TM_{0,1,0}$ mode, in the CSIW resonator is chosen as 7.9 GHz. Hence, the radius of the circular resonator can be obtained from (2) as $R_{eff}=9.78mm$. In order to improve the accuracy of the extraction results, the adjacent frequency interval ($\frac{(f_n-f_{n-1})}{0.5(f_n+f_{n-1})}*100\%$) among the selected modes exceeds 15%. The highest mode is chosen as the $TM_{4,4,0}$ mode whose resonating frequency is 58.431 GHz. Two planar circuits shown in Fig. 1 are designed for the extraction process. All the geometries of the two designed CSIW resonators are the same, except their thicknesses, which are 0.254 mm and 0.508 mm, respectively. The dimensions of the designed circuits are shown in Table I, and two fabricated prototypes are shown in Fig. 3. An Anritsu test fixture SC5225 and a Keysight VNA have been used to measure the S_{21} responses of those two circuits, which are shown in Fig.4 (a) and (b), respectively.

As shown in Fig. 4, the two measured transmission coefficients have almost the same resonant pattern due to the same radius of CSIW resonator. However, their magnitudes differ by at least 10 dB. Thicker resonator has a higher unloaded Q-factor than that of thinner resonator at the same resonating frequency, which leads to a higher magnitude of S_{21} even with a weak excitation shown in Fig. 4(b). It should be noticed that a larger S_{21} is obtained at higher frequency. This is resulted by the high-order resonating mode which has a much high quality factor than that of the fundamental mode. This would be very useful for high frequency measurement because measured S_{21} may be too low to be accepted if a fundamental mode is adopted in the extracting process.

Table II compares the extracted resonating frequencies of different resonating modes from the full-wave simulated and measured results. In the simulation, the relative dielectric constant always keeps unchanged as 2.2, while it may be varied along with operating frequency in the experiment. Hence, the simulation can be used as a reference for the experimental extraction. In addition, it can be noticed that there exists a small discrepancy between the resonating frequencies of 0.254 mm and 0.508 mm thick CSIW cavities for both cases of simulation and measurement. This is resulting from the different quality factors of the CSIW cavities. Generally, higher quality factor leads to sharper resonating peaks and a more accurate extraction result. However, thicker substrate requires a wider 50 ohm GCPW for excitation. When the extraction bandwidth is extremely wide, a wide 50 ohm GCPW needs to be avoided to keep that only the quasi-TEM mode is propagated along the GCPW for circuit excitations.

Table III presents the extracted equivalent dielectric characteristics of the TLY-5Z substrate and the effective conductivity of copper in PCB process. These are illustrated in Fig. 5 together with the equivalent dielectric loss tangent of Taconic TLY-5. As expected, the effective conductivity decrease as the operating frequency increases, while the equivalent loss tangent is increased. As shown in Fig. 5. (c), the extracted dielectric constant of the PCB keeps unchanged as 2.2 within 8-60 GHz.

B. EXTRACTION OF THE ELECTRICAL PROPERTIES OF THE TLY-5Z PCB WITHIN V-BAND AND W-BAND

As discussed above, since the conventional SMA only supports an operating frequency below 60 GHz, the waveguide interface is adopted to extract the equivalent dielectric characteristics and conductivity of PCB for operating frequencies beyond 60 GHz. Since the V-band extraction process is similar to that of the W-band extraction process, only W-band extraction process is discussed in detail in the rest of this part. Fig. 6 shows the circuit model for the extraction of the V- and W- bands and the corresponding geometries are presented in Table IV and V, respectively. The

This article has been accepted for publication in a future issue of this journal, but has not been fully edited. Content may change prior to final publication. Citation information: DOI 10.1109/ACCESS.2019.2911616, IEEE Access

TABLE II
EXTRACTED RESONANT FREQUENCIES WITHIN 8-60 GHZ

Resonant mode	ν_{mn}	Extracted from Simulations (GHz)		Extracted from experiments (GHz)	
		0.254mm	0.508mm	0.254mm	0.508mm
TM010	2.4048	7.965	7.977	7.9013	7.9581
TM110	3.8317	12.692	12.702	12.6088	12.6788
TM210	5.1356	17.016	17.021	16.9138	16.9659
TM020	5.5201	18.316	18.331	18.1913	18.3006
TM310	6.3802	21.149	21.165	21.0041	21.1156
TM120	7.0155	23.255	23.265	23.1172	23.2222
TM410	7.5883	25.156	25.171	25.0006	25.1187
TM220	8.4172	27.909	27.922	27.7372	27.8619
TM320	9.7610	32.348	32.351	32.1734	32.3178
TM130	10.1735	33.741	33.757	33.5384	33.6063
TM420	11.0647	36.710	36.715	36.4113	36.5763
TM040	11.7915	38.538	38.553	38.2881	38.4531
TM330	13.0152	43.166	43.169	42.8937	43.0875
TM430	14.3725	47.639	47.657	47.3687	47.4223
TM530	15.7002	51.675	51.702	51.2263	51.4619
TM440	17.6160	58.424	58.431	57.9416	58.1772

TABLE III
EXTRACTED EFFECTIVE RELATIVE DIELECTRIC CONSTANT AND EQUIVALENT CONDUCTIVITY WITHIN 8-60 GHZ

Resonant mode	Effective relative dielectric constant		Equivalent conductivity	
	0.254mm	0.508mm	0.254mm	0.508mm
TM010	2.2357	2.2107	2.1858E+07	2.2015E+07
TM110	2.2293	2.2084	1.7396E+07	1.7492E+07
TM210	2.2280	2.2061	1.4862E+07	1.4948E+07
TM020	2.2306	2.2076	1.3606E+07	1.3688E+07
TM310	2.2305	2.2107	1.1889E+07	1.1952E+07
TM120	2.2273	2.2083	1.1367E+07	1.1424E+07
TM410	2.2276	2.2094	1.0528E+07	1.0578E+07
TM220	2.2275	2.2093	9.1431E+06	9.1863E+06
TM320	2.2277	2.2102	8.8113E+06	8.8547E+06
TM130	2.2267	2.2099	8.8832E+06	8.9287E+06
TM420	2.2250	2.2041	8.9790E+06	9.0246E+06
TM040	2.2271	2.2107	8.5700E+06	8.6154E+06
TM330	2.2280	2.2085	8.2767E+06	8.3141E+06
TM430	2.2301	2.2121	7.8845E+06	7.9231E+06
TM530	2.2301	2.2107	7.0929E+06	7.1255E+06
TM440	2.2300	2.2112	6.5337E+06	6.5656E+06

TABLE IV
DIMENSIONS OF THE CSIW RESONATORS AT W-BAND (UNIT: MM)

W_siw	*L_siw*	*R*	*d*	*W_slot*	*L_slot*	*L_dis*
2.2	*10.4*	*6*	*0.3*	*0.4*	*0.6*	*1.4*

TABLE V
DIMENSIONS OF THE CSIW RESONATORS AT V-BAND (UNIT: MM)

W_siw	*L_siw*	*R*	*d*	*W_slot*	*L_slot*	*L_dis*
2.6	*10.4*	*8.19*	*0.3*	*0.5*	*0.8*	*1.8*

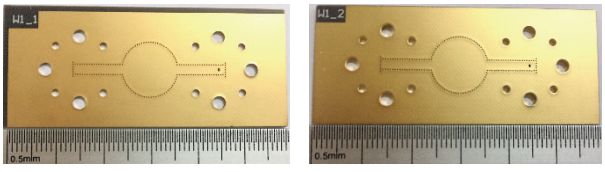

(a) (b)

FIGURE 7. Photographs of fabricated prototypes for the W-band

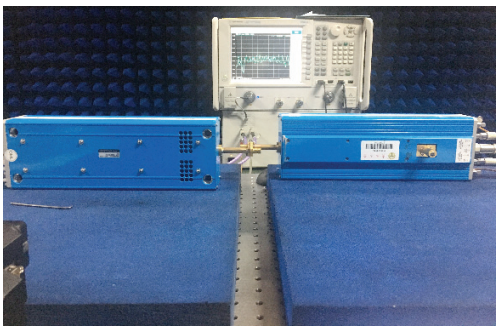

FIGURE 8. Measurement setup for the W-band extraction.

CSIW resonator is excited by the standard rectangular waveguide (WR10) at the input/output ports through SIW transmission lines within W band. Due to the operating

frequency bandwidth limitation of the standard WR10 waveguide, the extracted frequency is limited within 75-110 GHz.

Different to the extraction process in the part A where a fundamental resonating mode is adopted for the lowest frequency, a high-order resonating mode is selected in this process for the lowest frequency around 75.0 GHz due to the fundamental mode has a poor quality factor at such high frequency. Consequently, the TM_{430} mode is selected with a resonating frequency of around 78.0 GHz for the extraction at the lowest frequency. Hence, the effective and physical radiuses of CSIW resonant, i.e., R_{eff} and R, can be obtained as 5.91mm and 6mm from (2)-(5). Then, the TM_{160} mode is adopted for the highest frequency extraction, which has a resonating frequency around 108.0 GHz. Similarly, two circuits with the same CSIW resonators but different thicknesses have been used for the extraction process. As explained above, thick substrates have been used for improving the quality factor of the CSIW resonator as well as improving the extraction accuracy, whose thicknesses are 0.508 mm and 1.016 mm, respectively

Photographs of the fabricated two prototypes at W band are presented in Fig. 7, and the Keysight VNA is used to measure individually the S_{21} responses of those two prototypes with the WR10 interfaces, as shown in Fig. 8. By using the proposed method, the extracted resonant frequencies from full-wave simulated and measured results are presented in Table VI. Because the designed resonators can provide enough high quality factors, almost same resonant frequencies can be found in Table VI for each resonating modes in CSIW resonators with different thicknesses. The extracted equivalent complex dielectric permittivity and effective conductivity are presented in Table VII.

Similarly, two CSIW cavities are designed for the V-band extraction, in which the TM_{150} mode and TM_{250} mode are selected with resonating frequencies of 65.5 GHz and 71.0 GHz for the lowest and the highest frequency, respectively. The results of extraction at V band and W band are illustrated in Fig. 9. With the increasing of the operating frequency, the dielectric substrate loss increases quickly, and the effective conductivity of the copper used in the PCB process becomes worse. However, the TLY-5Z substrate has a very stable relative dielectric constant, even at 108 GHz.

IV. DISCUSSIONS

The overall extracted results from 8-110 GHz for the TLY-5Z substrate based PCB are plotted in Fig.10. It can be seen from Fig.10 (a) and (c) that the conductivity of the PCB under test drops from 8 to 110 GHz, while the dielectric loss increases monotonously as the frequency increases. In addition, the TLY-5Z substrate has a stable relative dielectric constant of 2.2 within 8-110 GHz, as illustrated in Fig.10 (c).

It should be mentioned that different substrate thicknesses and resonating modes have been adopted for the extraction of three frequency-bands mentioned above. That is based on the following criteria:

(a) *The choice of the substrate thickness*. Generally, a CSIW cavity with a thicker substrate has a higher quality factor which leads to a more accurate extraction result. On the one hand, the substrate thickness should be less than half-wavelength to avoid the appearance of TM_{mnp} mode ($p \neq 0$). For example, the selected substrate thicknesses at the W-band

TABLE VI
Extracted Resonant Frequencies within W-band

Resonant mode	ν_{mn}	Extracted from Simulations (GHz)		Extracted from Experiments (GHz)	
		h1=0.508mm	h2=1.0168mm	h1=0.508mm	h2=1.016mm
TM430	14.37254	78.119	78.146	78.0121	78.1286
TM530	15.70017	85.18	85.19	84.9293	85.1536
TM340	16.22347	89.148	89.211	88.9943	89.1764
TM920	17.24122	95.082	95.15	94.9529	95.1829
TM730	18.28758	99.374	99.261	99.27	99.4986
TM350	19.40942	105.01	105.047	104.8741	105.1534
TM160	19.61586	108.126	108.19	108.0669	108.2825

TABLE VII
Extracted Equivalent Relative Dielectric Constant and Effective Conductivity within W-band

Resonant mode	Equivalent relative dielectric constant		Effective conductivity	
	h1=0.508mm	h2=1.016mm	h1=0.508mm	h2=1.016mm
TM430	2.2074	2.2043	4.9220E+06	4.9144E+06
TM530	2.2125	2.2023	4.6262E+06	4.6140E+06
TM340	2.2103	2.2021	4.6367E+06	4.6204E+06
TM920	2.2145	2.1996	4.4370E+06	4.4206E+06
TM730	2.2061	2.2012	4.2264E+06	4.2167E+06
TM350	2.2130	2.2028	4.2122E+06	4.1999E+06
TM160	2.2141	2.2094	4.1167E+06	4.0956E+06

This article has been accepted for publication in a future issue of this journal, but has not been fully edited. Content may change prior to final publication. Citation information: DOI 10.1109/ACCESS.2019.2911616, IEEE Access

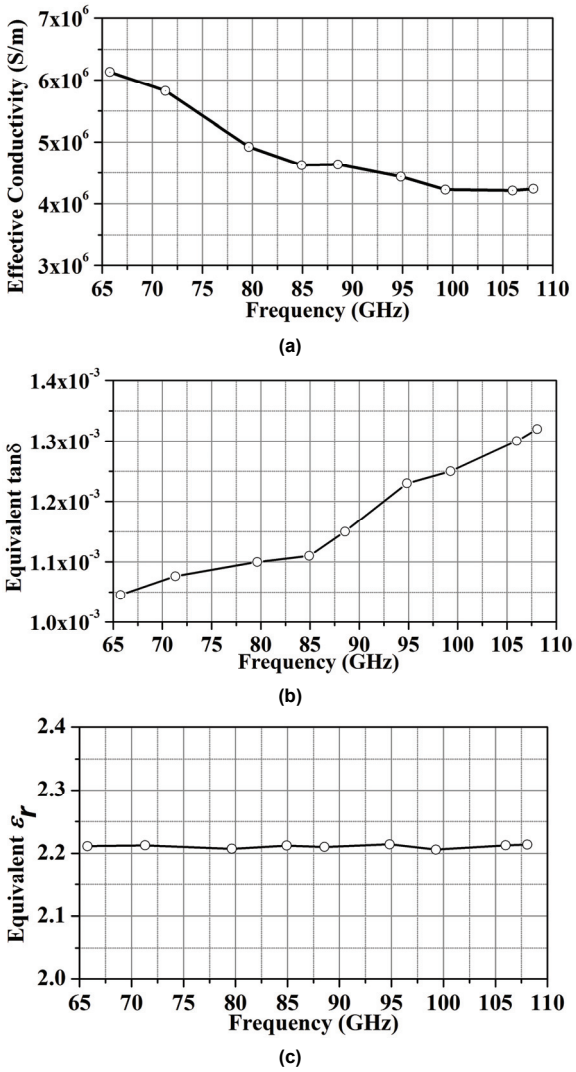

FIGURE 9. **Extracted equivalent dielectric properties and conductivity of a TYL-5Z PCB within V-band and W-band; (a) Effective conductivity; (b) Dielectric loss tangent; (c) Relative dielectric constant from *h*=0.508 mm thick substrate.**

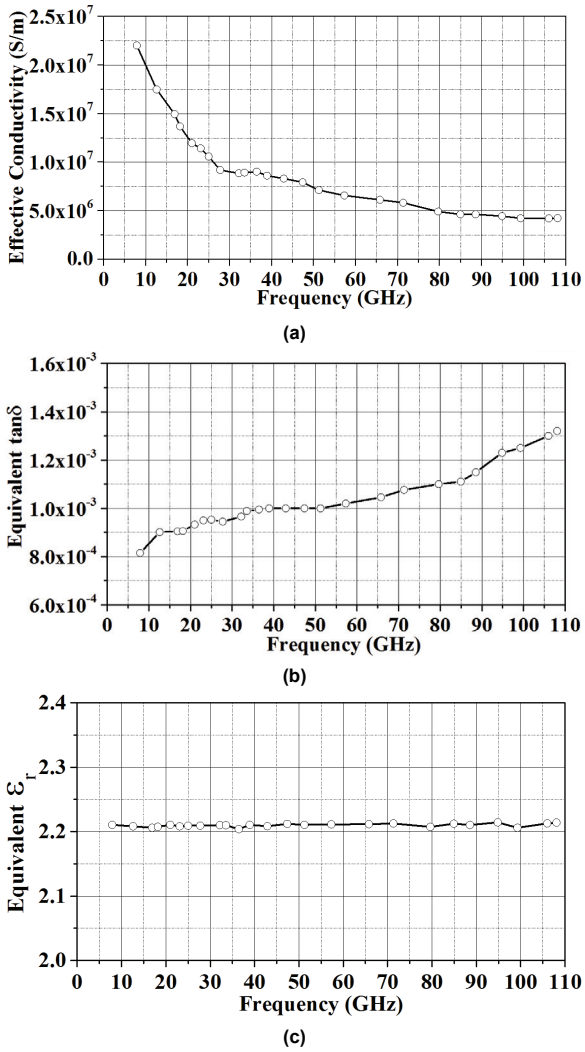

FIGURE 10. **Measured Printed-Circuit-Board Properties: (a) Effective conductivity; (b) Dielectric loss tangent; (c) Relative dielectric constant from *h*=0.508 mm thick substrate.**

TABLE VIII
COMPARISONS BETWEEN PROPOSED AND REPORTED EXTRACTION METHODS

Reference	Cavity type	Extraction BW (GHz)	Limitation of f_H/f_L	Cavity number	Excitation form
[18]	RSIW	12-19	<1.58	2	Microstrip
		16-26	<1.63	2	Microstrip
[19]	RSIW	89-105	<1.18	8	Waveguide
[20]	RSIW	60-110	<1.83	13	GSG
[21]	RSIW	28-40	<1.43	1	Waveguide
		75-110	<1.47	1	Waveguide
This work	CSIW	8-60	~7.5	1	GCPW
		75-110	<1.47	1	Waveguide

TABLE IX
DIMENSIONS OF THE FILTERS (Unit: MM)

W_1	W_2	W_3	W_4	L_1	L_2	L_3
0.76	4	5.1	4.9	3	11.95	12.45

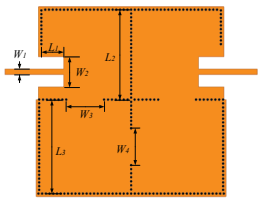

FIGURE 11. **Configuration of the fourth order Chebyshev filter.**

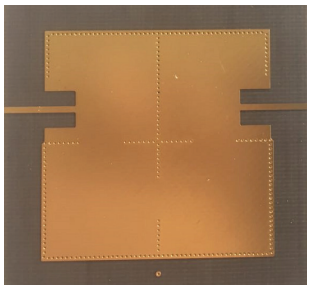

FIGURE 12. **Photograph of the fabricated filter.**

This article has been accepted for publication in a future issue of this journal, but has not been fully edited. Content may change prior to final publication. Citation information: DOI 10.1109/ACCESS.2019.2911616, IEEE Access

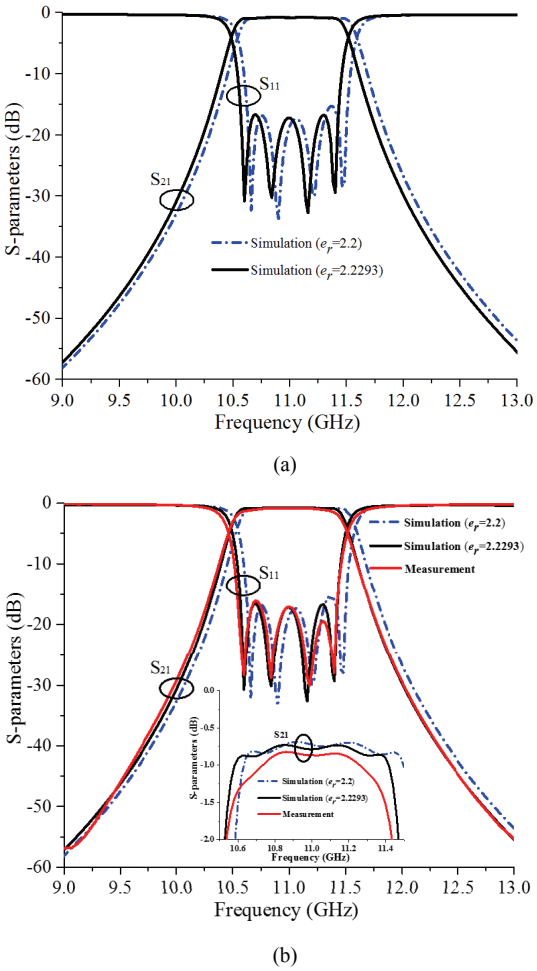

FIGURE 13. Simulated and measured S-parameters. (a) Simulation; (b) Measurement.

are 0.508 mm and 1.016 mm in this paper because one half-wavelength at 100 GHz in a CSIW cavity is about 1.011 mm. In addition, the selected substrate thickness should keep the excitation port only supports single-mode excitation. For example, GCPW can not keep a good transmission from 8 to 60 GHz when the substrate thickness is 1.016mm due to a too wide 50 ohm GCPW. Therefore, the selected substrate thicknesses from 8 to 60 GHz are 0.254mm and 0.508mm, respectively.

(b) *The selection of the operation modes.* The high-order mode can provide a high quality factor. However, the higher the high-order modes adopted, the smaller the separation among those high-order modes. That would lead to a narrow band extraction. Hence, at low frequency band, a relative lower-order mode can be chosen for achieving a wideband extraction, for example, the fundamental mode, i.e., $TM_{0,1,0}$, is chosen for a wideband extraction from 8 to 60 GHz. At higher frequency band, since the quality factor of the low-order mode is too small, a high-order mode should be chosen.

The extraction errors of the proposed method are mainly from the fabrication tolerance and the installation error of the measurement, especial for high millimeter-wave frequency extraction. As can be seen from (13)-(18), the effective radius of the CSIW resonator, i.e. R_{eff}, plays an important role in the extraction process. As an example, the extracted results at 12.61 GHz from the measured S_{21} of the 0.508 mm thick TLY-5 substrate based PCB are $\varepsilon_r = 2.208$, $\sigma_{eff} = 1.749E + 07\ S/m$ and $\tan\delta = 9.01E - 04$. When the radius of the CSIW resonator increases by 0.02mm (0.2%), the extracted equivalent dielectric constant rises 0.363% to 2.216, the effective conductivity drops 3.15% to 1.694E+07 S/m and the dielectric loss tangent reduces 1.62% to 8.864E-04. These errors caused by fabrication tolerance are acceptable. As for the installation error of the measurement, it can be reduced by multiple measurements.

Table VIII summarizes the comparison between this proposed and reported extraction methods. In order to extract the electrical characteristics of PCB within 8-60 GHz, at least three groups of RSIW resonators are required by the traditional resonator methods. The proposed method overcomes the limitation of frequency bandwidth of RSIW resonators and accurately extracts extremely wideband complex dielectric permittivity and effective conductivity by using one pair of CSIW resonators. In addition, the proposed method has lower costs and less measurement errors.

V. EXPERIMENTAL VERIFICATIONS

Based on the extracted results of TLY-5Z substrate with thickness of 0.254mm, a fourth order Chebyshev filter is designed at X band. The topological structure is presented in Fig. 11 and the dimensions are listed in table IX. As shown in Fig. 12, the filter is fabricated and measured by using the Keysight Vector Network Analyzer (VNA) and the Anritsu Test Fixture SC5225.

From Fig. 13 (a), compared with the responses of the filter based on the extracted results of TLY-5Z substrate, the responses of the filter designed on the substrate with relative dielectric constant of 2.2 shift 70MHz to the high frequency. In Fig. 13 (b), the measured results of the fourth order Chebyshev filter are in excellent agreement with the simulated results of the filter based on the extracted results. The insertion loss error between the simulation and measurement is around 0.08 dB at 11 GHz. The error is mainly caused by the fabrication tolerance. In addition, the test fixture has a radiation loss, which becomes worse at high frequency band. Therefore, it can be concluded that the extraction of electrical characteristics of PCB guides to accurately design microwave and millimeter-wave filters.

VI. CONCLUSION

In this paper, by utilizing the wideband resonating frequency distribution of multiple high-order TM_{mn0} modes in a CSIW cavity, the equivalent dielectric loss, metal loss, and relative dielectric constant of PCB can be separately extracted over an extremely wide frequency band by only using a small number of CSIW resonators. Comparing with the conventional method, the proposed method has higher efficiency, lower

costs and less measurement errors. Experiments, which extract the equivalent dielectric characteristics and conductivity of a TLY-5Z substrate based printed circuit board within 8-110 GHz, have demonstrated the merits of the proposed method. In addition, it should be mentioned, since the proposed method is based on the resonator-extraction method, it would be failed if a very high lossy substrate or a metal needs to be investigated because it is very hard to discriminate the resonating peaks from measured S_{21} results for the extraction due to a very low quality factor for that case.

REFERENCES

[1] Y. Tang, K. Wu, and N. K. Mallat, "Development of substrate-integrated waveguide filters for low-cost high-density RF and microwave circuit integration: direct-coupled cavity bandpass filters with Chebyshev response," *IEEE Access*, vol. 63, no. 3, pp. 1313-1325, July. 2015.

[2] M. Kheir, T. Kröger, and M. Höft, "A new class of highly-miniaturized reconfigurable UWB filters for multi-band multi-standard transceiver architectures," *IEEE Access*, vol. 5, pp. 1714–1723, Feb. 2017.

[3] Z.-C. Guo, S.-W. Wong, J.-Y. Lin, L. Zhu, Q.-X. Chu, Q. Zhang, and Y. Yang, "Triple-mode cavity bandpass filter on doublet with controllable transmission zeros," *IEEE Access*, vol. 5, pp. 6969–6977, 2017.

[4] M. Soltani, M. Freyburger, R. Kulkarni, R. Mohr, T. Groezinger, and A. Zimmermann, "Reliability study and thermal performance of LEDs on molded interconnect devices (MID) and PCB," *IEEE Access*, vol. 6, pp. 51669–51679, Sep. 2018.

[5] J, Li, J. Shi, L. Li, T. A. Khan, J. Chen, Y. Li, and A. Zhang, "Dual-band annular slot antenna loaded by reactive components for dual-sense circular polarization with flexible frequency ratio," *IEEE Access*, vol. 6, pp. 64063–64070, Oct. 2018.

[6] Z. C. Hao, X. M. Liu, X. P. Huo, and K. K. Fan, "Planar high-gain circularly polarized element antenna for array applications," *IEEE Trans. Antennas Propag.*, vol. 63, no. 5, pp. 1937-1948, May. 2015.

[7] Z. C. Hao, W. Q. Ding, and W. Hong, "Developing low-cost W-Band SIW bandpass filters using the commercially available printed-circuit-board technology," *IEEE Trans. Microw. Theory Techn.,* vol. 64, no. 6, pp. 1775-1786, Jun. 2016.

[8] J. F. Xu, Z. N. Chen, X. M. Qing, and W. Hong, "140-GHz planar broadband LTCC SIW slot antenna array," *IEEE Trans. Antennas Propag.*, vol. 60, no. 6, pp. 3025-3028, Jun. 2012.

[9] W. C. Yang, Y. Y. Yang, W. Q. Che, C. Fan, and Q. Xue, "94-GHz compact 2-D multibeam LTCC antenna based on multifolded SIW beam-forming network," *IEEE Trans. Antennas Propag.*, vol. 65, no. 8, pp. 4328-4333, Aug. 2017.

[10] A. Nafe and F. Ghaffar, "A ferrite LTCC-based monolithic SIW phased antenna array," *IEEE Trans. Antennas Propag.*, vol. 65, no. 1, pp. 196-205, Jan. 2017.

[11] Z. W. Miao, Z. C. Hao, G. Q. Luo, J. Wang, X. Wang, and W. Hong, "140 GHz high-gain LTCC-integrated transmit-array antenna using a wideband SIW aperture-coupling phase delay structure," *IEEE Trans. Antennas Propag.*, vol. 66, no. 1, pp. 182-190, Jan. 2018.

[12] K.-X. Wang, X.-F. Liu, Y.-C. Li, L.-Z. Lin, and X.-L. Zhao, "LTCC filtering rat-race coupler based on eight-line spatially-symmetrical coupled structure," *IEEE Access*, vol. 6, pp. 262–269, 2018.

[13] K.-W. Qian, G.-L. Huang, J.-J. Liang, B. Qian, and Tao. Yuan, "An LTCC interference cancellation device for closely spaced antennas decoupling," *IEEE Access*, vol. 6, pp. 68255–68262, 2018.

[14] L. Zhao, F. Liu, X. Shen, G. Jing, Y.-M. Cai, and Y. Li, "A highpass antenna interference cancellation chip for mutual coupling reduction of antennas in contiguous frequency bands," *IEEE Access*, vol. 6, pp. 38097–38105, Jul. 2018.

[15] F. Fesharaki, C. Akyel, and K. Wu, "Broadband permittivity measurement of dielectric materials using discontinuity in substrate integrated waveguide," *Electron. Lett.,* vol. 49, no. 3, pp. 194-196, Jan. 2013.

[16] X. Wang and A. Stelzer, "Millimeter-wave material characterization using laminated waveguides," *IEEE Trans. Microw. Theory Techn.,* vol. 62, no. 8, pp. 1762-1771, Aug. 2014.

[17] C. Jones, "Permittivity and permeability measurements using stripline resonator cavities-a comparison," *IEEE Trans. Instrum. Meas.*, vol. 48, no. 4, pp. 843-848, Aug. 1999.

[18] X. C. Zhu, W. Hong, P. P. Zhang, Z. C. Hao, H. J. Tang, K. Gong, J. X. Chen, and K. Wu, "Extraction of dielectric and rough conductor loss of printed circuit board using different method at microwave frequencies," *IEEE Trans. Microw. Theory Techn.,* vol. 63, no. 2, pp. 494-503, Feb. 2015.

[19] Y. J. Cheng, and X. L. Liu, "W-band characterizations of printed circuit board based on substrate integrated waveguide multi-resonator method," *IEEE Trans. Microw. Theory Techn.,* vol. 64, no. 2, pp. 599-606, Feb. 2016.

[20] D. E. Zelenchuk, V. Fusco, G. Goussetis, A. Mendez, and D. Linton, "Millimeter-wave printed circuit board characterization using substrate integrated waveguide resonators," *IEEE Trans. Microw. Theory Techn.*, vol. 60, no. 10, pp. 3300-3308, Oct. 2012.

[21] H. B. Wang, and Y. J. Cheng, "Broadband printed-circuit-board characterization using multimode substrate-integrated-waveguide resonator," *IEEE Trans. Microw. Theory Techn.,* vol. 65, no. 6, pp. 2145-2152, Jun. 2017.

[22] S. C. Chen, M. C. Guo, K. W. Xu, P. Zhao, Y. Hu, L. X. Dong, and G. F. Wang, "A dielectric constant measurement system for liquid based on SIW resonator," *IEEE Access*, vol. 6, pp. 41163–41172, July. 2018.

[23] D. Y. Kim, W. S. Chung, C. H. Park, S. J. Lee, and S. Nam, "A series slot array antenna for 45°-inclined linear polarization with SIW technology," *IEEE Trans. Antennas Propag*., vol. 60, no. 4, pp. 1785-1795, Apr. 2012.

[24] Y. J. Li and K. M. Luk, "60-GHz substrate integrated waveguide fed cavity-backed aperture-coupled microstrip patch antenna arrays," *IEEE Trans. Antennas Propag*., vol. 63, no. 3, pp. 1075-1085, Mar. 2015.

[25] Q. L. Yang, Y. L. Ban, K. Kang, C. Y. D. Sim, and G. Wu, "SIW multibeam array for 5G mobile devices," *IEEE Access*, vol. 4, pp. 2788–2796, Jun. 2016.

[26] Q.-L. Yang, Y.-L. Ban, J.-W. Lian, Z.-F. Yu, and B. Wu, "SIW butler matrix with modified hybrid coupler for slot antenna array," *IEEE Access*, vol. 4, pp. 9561–9569, Dec. 2016.

[27] M. Abdallah, Y. Wang, W. A. Wahab, and S. S. Naeini, "Design and optimization of SIW center-fed series rectangular dielectric resonator antenna array with 45° linear polarization," *IEEE Trans. Antennas Propag.*, vol. 66, no. 1, pp. 23-31, Jan. 2018.

[28] Z. Gan, Z.-H. Tu, and Z.-M. Xie, "Pattern-reconfigurable unidirectional dipole antenna array fed by SIW coupler for millimeter wave application," *IEEE Access*, vol. 6, pp. 22401–22407, Feb. 2018.

[29] X. Li, J. Xiao, Z. Qi, and H. Zhu, "Broadband and high-gain SIW-fed antenna array for 5G applications," *IEEE Access*, vol. 6, pp. 56282–56289, Oct. 2018.

[30] J. X. Zhuang, Z. C. Hao, and W. Hong, "Silicon micromachined terahertz bandpass filter with elliptic cavities," *IEEE Trans. THz Sci. Technol.*, vol. 5, no. 6, pp.1040-1047, Nov. 2015.

[31] Y. W. Wu, Z. Z. Hao, M. C. Tao, and W. Hong, "Extracting extremely wideband complex dielectric permittivity and effective conductivity by using one pair of SIW circular cavities," in *IEEE International Wireless Symposium*, 2018.

[32] J. Gu, Y. Fan, Y. H. Zhang, "A low-loss SICC filter using LTCC technology for X-band application," *Applied Superconductivity and Electromagnetic Devices*, *2009. ASEMD 2009. International Conference on*, pp.152-154, 25-27, Sep. 2009.

[33] Z.-C. Hao, W.-Q. Ding, and W. Hong, "Developing low-cost W-band SIW bandpass filters using the commercially available printed-circuitboard technology," *IEEE Trans. Microw. Theory Techn*., vol. 64, no. 6, pp. 1775–1786, Jun. 2016.

[34] J. M. Fu, "Microwave resonator," in *Advanced Electromagnetic Theory,* 1st ed., vol. 7, Xi'an, China: Xi,an Jiaotong University Press, 2000, pp. 201-202.

[35] DataSheet for the TLY-5Z substrate; [Online]. Available: http://www.4taconic.com/uploads/ADD%20Data%20Sheets/1510763061_Taconic%20TLY-5Z%20Technical%20Data%20Sheet.pdf

[36] Ansiru Test Fixture wensite; [Online]. Available: https://www.anritsu.com/zh-cn/components-accessories/products/3680-series